ELSEVIER

Journal of Electrostatics 50 (2001) 177–190

Journal of
ELECTROSTATICS

www.elsevier.nl/locate/elstat

# Theoretical model of electrostatic precipitator performance for collecting polydisperse particles

S.H. Kim, H.S. Park, K.W. Lee*

*Department of Environmental Science and Engineering, Kwangju Institute of Science and Technology, 1 Oryong-dong, Puk-gu, Kwangju 500-712, South Korea*

Received 11 August 1999; received in revised form 30 April 2000; accepted 6 November 2000

**Abstract**

This paper presents a theoretical model for predicting the collection performance of an electrostatic precipitator (ESP) for polydisperse particles. The particle size distribution of polydisperse particles was represented by a lognormal function, and then the statistical method of moments was employed to obtain a set of the first three moment equations. The continuous evolution of the particle size distribution in an ESP is taken into account with the first three moment equations. The employed model was validated by comparing its predictions with existing experimental data and other theoretical prediction models. The effects of the particle size distribution on the ESP performance were examined. The results indicated that both overall mass and number efficiencies were higher for aerosols with a larger geometric mean diameter and a lower geometric standard deviation. © 2001 Elsevier Science B.V. All rights reserved.

*Keywords:* Electrostatic precipitator; Polydisperse particles; Lognormal distribution; Particle collection

## 1. Introduction

Electrostatic precipitators (ESPs) are one of the most common particulate control devices used to control fly ash emissions from utility boilers, incinerators and many industrial processes. They have many advantages of operating in a wide range of gas temperature and achieving high particle collection efficiency compared with mechanical devices such as cyclones and bag filters. Theoretical ESP performance models for

* Corresponding author. Tel.: + 82-62-970-2438 e2432; fax: + 82-62-970-2434.
*E-mail address:* lee@kjist.ac.kr (K.W. Lee).

0304-3886/01/$ - see front matter © 2001 Elsevier Science B.V. All rights reserved.
PII: S0304-3886(00)00035-8

monodisperse particles were suggested by many researchers such as Deutsch [1], Cooperman [2], Leonard et al. [3] and Zhibin and Guoquan [4].

The first mathematical model of ESP performance is the Deutsch–Anderson model [1]. Although the Deutsch–Anderson model has been widely used for the design of ESPs, the assumption of an infinite transverse turbulent dispersion was overly restrictive to provide accurate prediction. Other researchers tried to explain particle diffusion process as well as electrostatic force in the ESPs. Specifically, Cooperman [2] considered the particle re-entrainment and the longitudinal turbulent mixing effects, Leonard et al. [3] the finite turbulent diffusion coefficient, and Zhibin and Guoquan [4] the non-uniform air velocity profile and the turbulent mixing coefficient. Although the polydisperse nature of particles can be accounted for by the integration of grade efficiency, the continuous change of particle size distribution along the ESP may not be easily considered with the above theoretical models. Bai et al. [5] developed a moment model approximating the particle size distribution by a lognormal function through the ESP. The Bai et al. [5] model described continuous evolution of the particle size distribution along the ESP for predicting the mass and number efficiencies. With minimal computing, this model gives information on average properties of the particle size distribution such as total particle number concentration, average particle size and polydispersity. This model has proved useful in predicting ESP performance for collecting polydisperse particles. However, Bai et al. [5] considered flow convection and electrostatic force without particle diffusion process into the collection plates. Since the turbulent diffusion process is one of the main mechanisms which dominate the behavior of aerosol particles in ESP [2], it should be involved to provide more accurate prediction of an ESP performance.

Therefore, the goal of this paper is to present a modified model for considering simultaneously the convection force, the electrostatic force, and the diffusion to predict the wire–plate ESP performance for collecting polydisperse particles. The performance of the present model is verified by comparing its predictions with other theoretical models and with existing experimental data. The continuous evolution of particle size distribution along a wire–plate ESP and its effects on the ESP performance are also studied and quantitatively determined.

## 2. Theoretical model development

### *2.1. Basic assumptions*

The following major assumptions are made in developing the proposed model to study the performance of an ESP:

1. The system is in a steady-state operating condition.
2. Electrical resistivity of particles is not considered in this model.
3. Non-ideal effects such as leakage and rapping re-entrainment are neglected.
4. The flow is a plug flow with uniform velocity corresponding to the mean velocity of a fully developed turbulent flow.

5. The particle size distribution is preserved as a lognormal function throughout the ESP, although the three parameters, the total number, the geometric standard deviation and the mean radius are allowed to vary.
6. The mobility of charged particle is constant in every small increment of an ESP.
7. The fluctuation of electric force and the particle space-charge effect are neglected.

### 2.2. Electric field equation

The following governing equations and numerical method of McDonald et al. [6] are applied to obtain electric field strength in the presence of the space charge as follows:

$$\nabla^2 V = -\frac{\rho_e}{\varepsilon_0}, \tag{1}$$

$$\rho_e^2 = \varepsilon_0(\nabla V)\cdot(\nabla \rho_e), \tag{2}$$

where $V$ is the electric potential, $\rho_e$ is the space-charge density, and $\varepsilon_0$ is the permittivity of free space. To solve the above two equations, the following boundary conditions are employed: $V = V_0$ at the wire, $V = 0$ along the collection plate, $\nabla V = 0$ along any symmetric planes, and $\rho_e = j_p[b(-\partial V/\partial y)]^{-1}$ near the collection plate. Here $V_0$ is the applied voltage, $j_p$ is the average current density at the collection plate without particles, and $b$ is the mobility of charged particles.

### 2.3. Mass balance equation

The schematic diagram of a wire–plate ESP is shown in Fig. 1. The simplest mass balance equation containing all of the fundamental forces is written as

$$U_{av}\frac{\partial N}{\partial x} - V_e\frac{\partial N}{\partial y} = D_1\frac{\partial^2 N}{\partial x^2} + D_2\frac{\partial^2 N}{\partial y^2}, \tag{3}$$

where $N$ is the number concentration of particles, $D_1$ and $D_2$ represent, respectively, the longitudinal and the transverse particle diffusion coefficients, $V_e$ the migration velocity, and $U_{av}$ the average flow velocity. This mass balance equation can be solved by the separation of variables method. The boundary conditions are given as follows:

$$N(0, y) = N_0,$$
$$N(x, y) \to 0 \quad \text{as } y \to \infty,$$
$$D_2\frac{\partial N}{\partial y} + V_e N = 0 \quad \text{at } y = 0,$$
$$D_2\frac{\partial N}{\partial y} = 0 \quad \text{at } y = \frac{W}{2}. \tag{4}$$

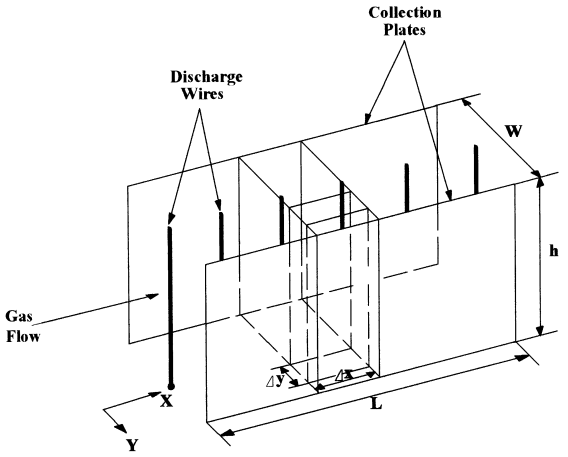


Fig. 1. Schematic diagram of a wire–plate electrostatic precipitator.

### 2.4. Diffusion coefficients

Careful examination of the derivations shows that approximation of the longitudinal and the transverse diffusion coefficients was used to obtain a simple efficiency formula as the following three cases:

*Case* I: $D_1 = 0$ *and* $D_2 = \infty$ (*Deutsch model* [1]). Bai et al. [5] assumed that the longitudinal mixing coefficient ($D_1$) is taken as zero and the transverse mixing coefficient ($D_2$) as infinity for improving the prediction of Deutsch–Anderson model [1]. Thus, the inlet particle distribution was assumed to be uniform. It is assumed that there is no particle diffusion process into the collection plate.

*Case* II: $D_1 \gg V_e L/2$ *and* $D_2 = 0$ (*Cooperman model* [2]). This case says that for very high longitudinal mixing, the concentration gradient sweeps particles out the outlet so fast that they do not have time to come near the plate. Though this case gives some clue about very high mixing conditions, it is too extreme to be used for actual design.

*Case* III: $V_e^2/D_2 \ll U_{av}^2/D_1, D_1 \cong D_2 < 50\,\mathrm{cm^2\,s^{-1}}$ (*Leonard et al. model* [3]). The present model is based on this case for improving the predictions of the Leonard et al. model [3]. Since the migration velocity for coarse particles, e.g. $> 10\,\mu\mathrm{m}$, is an order of magnitude smaller than the gas velocity, $V_e^2/D_2 \ll U_{av}^2/D_1$ is satisfied. With this assumption, Cooperman [2] suggested the unified efficiency theory from Eq. (1) as follows:

$$\frac{N}{N_0} = \frac{2\exp(V_e W/4D_2)}{\pi(V_e W/4D_2)} \exp\left(-\frac{V_e^2 x}{4U_{av} D_2}\right). \tag{5}$$

As noted, $D_1$ is absent and only $D_2$ plays a role. This implies that longitudinal mixing is dominated by gas velocity, but that transverse mixing has a role to play in enhancing the build-up of particles near the plate due to migration velocity [7]. The

concentration of particles along the ESP is obtained by differentiating Eq. (5):

$$\frac{\mathrm{d}N(r)}{\mathrm{d}x} = -\frac{V_e^2}{4U_{av}D_2}N(r). \tag{6}$$

In order to evaluate the particle diffusivity, the flow is assumed to be a fully developed turbulent channel flow. The related physical quantities are specified below [8,9]:

$$\frac{1}{f^{1/2}} = -1.8\log_{10}\left(\frac{6.9}{\mathrm{Re}}\right), \qquad U_\tau = \sqrt{\frac{fU_{av}^2}{8}},$$

$$D_t = 0.12U_\tau W, \qquad D_B = \frac{kTC_c}{6\pi\mu r}, \qquad D_p = D_t + D_B, \tag{7}$$

where $f$ is the friction factor, $\mu$ the gas viscosity, Re the Reynolds number ($= U_{av}W/\nu$), $\nu$ the kinetic viscosity, $U_\tau$ the friction velocity, $D_p(= D_2)$ the particle diffusivity, $D_t$ the turbulent diffusivity, $D_B$ the Brownian diffusivity and $C_c$ the Cunningham slip correction factor.

In turbulent flow, the order of Brownian diffusivity is much smaller than that of turbulent diffusivity. Thus, the particle diffusion coefficient was set to be equal to the turbulent particle diffusivity for simplified calculation. Once the migration velocity of particles is determined, the evolution of the particle size distribution function, $N(r)$, along an ESP can be solved using Eq. (6). The migration velocity of a particle of radius $r$ near the collecting plate is given by Bai et al. [5]:

$$V_e = \frac{qE_cC_c}{6\pi\mu r}, \tag{8}$$

where $q$ is the particle charge, $E_c$ the electric field strength at the collecting plate surface which is obtained from Eqs. (1) and (2) [6], and $C_c$ the Cunningham slip correction factor.

### 2.5. Particle charge equation

Particle charge is a function of particle size, and can be described by Cochet's charge equation:

$$q = 4\pi\varepsilon_0 Er^2\left[\left(1+\frac{\lambda_i}{r}\right)^2 + \frac{2}{1+\lambda_i/r}\frac{\kappa-1}{\kappa+2}\right], \tag{9}$$

where $\varepsilon_0$ is the permittivity of free space, $E$ the local electric field strength, $\lambda_i$ the ionic mean free path, and $\kappa$ the dielectric constant of particles.

Although Cochet's equation is simple compared to other particle charge theories, it is not an integrable form. Therefore, Cochet's equation is converted into an integrable form by the assumption of the Bai et al. [5]:

$$q = q_1 + q_2 r^2, \tag{10}$$

where $q_1 = 4\pi\lambda_i^2\varepsilon_0 E$ and $q_2 = 4[1 + 2(\kappa - 1)/(\kappa + 2)]\pi\varepsilon_0 E$, for the ionic mean free path less than particle radius.

### 2.6. Cunningham slip correction factor

Similarly, the Cunningham slip correction factor can also be converted into an integrable form by using the approximation proposed by Bai and Biswas [10]:

$$C_c = C^* + 3.314\lambda/(2r), \tag{11}$$

where $\lambda$ is the gas mean free path, $C^* = 0.56$ for $\lambda/(2r) > 1$ and $C^* = 1$ for $\lambda/(2r) \leqslant 1$.

### 2.7. Migration velocity

The local electric field strength ($E$) is here assumed to be equal to the average electric field strength ($E_{av}$) in a single-stage ESP [5,11]. Substituting Eqs. (10) and (11) into Eq. (8), the migration velocity is written as

$$V_e = q_1 q_4 r^{-2} + q_1 q_3 r^{-1} + q_2 q_4 + q_2 q_3 r, \tag{12}$$

where $q_3 = E_{av} C^*/(6\pi\mu)$ and $q_4 = 3.314\lambda_i E_{av}/(12\pi\mu)$.

### 2.8. Moment method

The use of moments has the advantage of simplicity in evaluating the continuous evolution of polydisperse particles. The $k$th moment of a particle size distribution is

$$M_k = \int_0^\infty r^k N(r)\,\mathrm{d}r. \tag{13}$$

While the size distribution function, $N(r)$, for lognormally distributed particles is defined as

$$N(r) = \frac{N_0}{\sqrt{2\pi} r \ln\sigma_g} \exp\left[ -\frac{\ln^2(r/r_g)}{2\ln^2\sigma_g} \right], \tag{14}$$

where $N_0$ is the total particle number concentration, $r_g$ is the geometric mean particle radius and $\sigma_g$ is the geometric standard deviation. Values of $r_g$ and $\sigma_g$ can be expressed in terms of the first three moments of the distribution as [12]

$$r_g = M_0^{-3/2} M_1^2 M_2^{-1/2}, \tag{15}$$

$$\ln^2\sigma_g = \ln\left(\frac{M_0 M_2}{M_1^2}\right). \tag{16}$$

The first three moments of the distribution are sufficient to describe the behavior of the size distribution of lognormally preserving particles and the $k$th moment of the

distribution can be written in terms of $M_0, r_g$ and $\sigma_g$ as

$$M_k = M_0 r_g^k \exp\left(\frac{k^2}{2} \ln^2 \sigma_g\right). \tag{17}$$

Substituting Eq. (12) into Eq. (6), multiplying both sides by $r^k$ and integrating over the entire particle size range, the continuous evolution of the first three moments of the distribution along the ESP are given by

$$\frac{dM_0}{dx} = -[a_1 M_0^{15} M_1^{-24} M_2^{10} + a_2 M_0^{10} M_1^{-15} M_2^6 + a_3 M_0^6 M_1^{-8} M_2^3 + a_4 M_0^3 M_1^{-3} M_2 + a_5 M_0 + a_6 M_1 + a_7 M_2], \tag{18}$$

$$\frac{dM_1}{dx} = -[a_1 M_0^{10} M_1^{-15} M_2^6 + a_2 M_0^6 M_1^{-8} M_2^3 + a_3 M_0^3 M_1^{-3} M_2 + a_4 M_0 + a_5 M_1 + a_6 M_2 + a_7 M_0 M_1^{-3} M_2^3], \tag{19}$$

$$\frac{dM_2}{dx} = -[a_1 M_0^6 M_1^{-8} M_2^3 + a_2 M_0^3 M_1^{-3} M_2 + a_3 M_0 + a_4 M_1 + a_5 M_2 + a_6 M_0 M_1^{-3} M_2^3 + a_7 M_0^3 M_1^{-8} M_2^6], \tag{20}$$

where $a_1 = q_1^2 q_4^2/a^*$, $a_2 = 2q_1^2 q_3 q_4/a^*$, $a_3 = (2q_1 q_2 q_4^2 + q_1^2 q_3^2)/a^*$, $a_4 = 4q_1 q_2 q_3 q_4/a^*$, $a_5 = (2q_1 q_2 q_3^2 + q_2^2 q_4^2)/a^*$, $a_6 = 2q_2^2 q_3 q_4/a^*$, $a_7 = q_2^2 q_3^2/a^*$ and $a^* = 4U_{av} D_t$.

The associated initial conditions for Eqs. (18)–(20) are

$$M_0 = N_0,$$
$$M_1 = N_0 r_{g0} \exp(0.5 \ln^2 \sigma_{g0}),$$
$$M_2 = N_0 r_{g0}^2 \exp(2 \ln^2 \sigma_{g0}) \quad \text{at } x = 0. \tag{21}$$

Eqs. (18)–(20), along with the initial conditions, constitute a set of coupled ordinary differential equations (ODEs) that describe the continuous evolution of the first three moments of the distribution along the ESP. These ODEs are then solved by the fourth-order Runge–Kutta method.

## 3. Results and discussion

The predictions were made based on the parameter values in Table 1 except for the purpose of comparison with the experimental data. The conservation of the lognormal particle size distribution in an ESP was investigated. Fig. 2 shows the evolution of the particle size distribution along an ESP. The inlet particle geometric mean radius ($r_{g0}$) and the geometric standard deviation ($\sigma_{g0}$) are 1 μm and 2.0, respectively. SCA

Table 1
Parameters used in the present theoretical model of an ESP performance

| Parameters | Values | Unit |
|---|---|---|
| Particle density | 2270 | $kg\,m^{-3}$ |
| $E_{av}$ | 5 | $kV\,cm^{-1}$ |
| $U_{av}$ | 1 | $m\,s^{-1}$ |
| $W$ | 0.4 | m |
| $\mu$ | $2.4\times10^{-5}$ | $kg\,m^{-1}$ |
| $\varepsilon_0$ | $8.85\times10^{-12}$ | $F\,m^{-1}$ |
| $\lambda$ | 0.065 | μm |
| $\lambda_i$ | 0.1 | μm |
| $\kappa$ | 5 | |

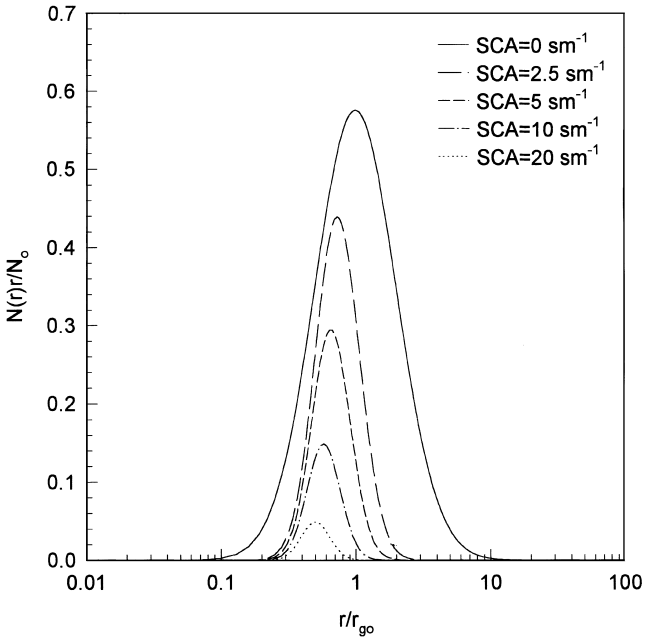


Fig. 2. Evolution of particle size distribution obtained by computing the grade efficiency of each size (inlet particle geometric mean radius and GSD were 1 μm and 2.0).

denotes the specific collection surface defined as the ratio of the total collection area to the total gas volume flow rate. That is to say, SCA $= 2x/U_{av}W$, where $x$ is longitudinal distance from the inlet, $U_{av}$ the average flow velocity, and $W$ the width between two collection plates. Therefore, the given SCA number is showing the precipitator length we considered. As can be seen, when starting with a lognormal inlet particle size distribution (SCA $= 0$), the distribution shifts continuously to the finer particles as SCA becomes larger. Overall size range of particles is collected efficiently by

electrostatic force and particle diffusion simultaneously. As a result, the particle size distribution remains in a lognormal form along an ESP without significant deviation. Fig. 3 shows the predicted overall number efficiencies as a function of particle radius with different $\sigma_{g0}$ values. The SCA and the inlet particle geometric mean radius were $25\,\mathrm{sm}^{-1}$ and 1 μm, respectively. As can be seen, the effects of particle diffusion process and electrostatic force are very significant for inlet particle geometric mean radius in the range of 0.01–1 μm. It is also seen that variations of the overall number efficiency of the Bai et al. [5] model with respect to particle polydispersity are similar to those obtained from the present model. For the typical range of geometric particle mean radius (0.05–5 μm) encountered in many industrial combustion processes, particle deposition will be enhanced by the predictions of the present model without considering the space-charge effect. Fig. 4(a) shows the overall number efficiencies as a function of SCAs with different $\sigma_{g0}$ values. For SCAs less than $3\,\mathrm{sm}^{-1}$, overall number efficiency increases with increasing particle polydispersity. However, the opposite trend is observed for SCAs larger than $3\,\mathrm{sm}^{-1}$. This is because the inlet particles with a wide spread (e.g., $\sigma_{g0} = 2.0$) tend to lose the coarse particles to the collector surface at a faster rate, which may lead to high collection efficiency at the early stages of an ESP. But as SCA increases, the uncollected particles are undergoing charging difficulty. Therefore, the particle collection rate slows down, and the overall number efficiency may become lower than that for inlet particles with narrow spread. If the geometric standard deviation is large, there are finer and coarser particles. The

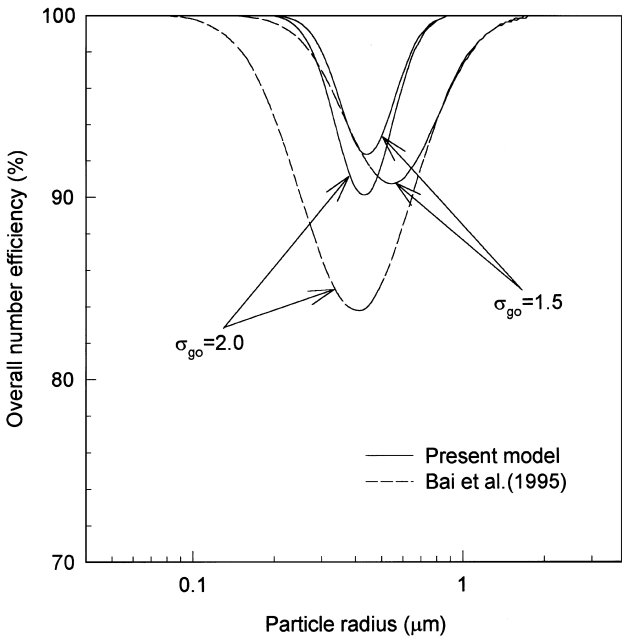


Fig. 3. Predicted overall number efficiencies as a function of particle radius with different $\sigma_{g0}$ values (SCA and inlet particle geometric mean radius were $25\,\mathrm{sm}^{-1}$ and 1 μm).

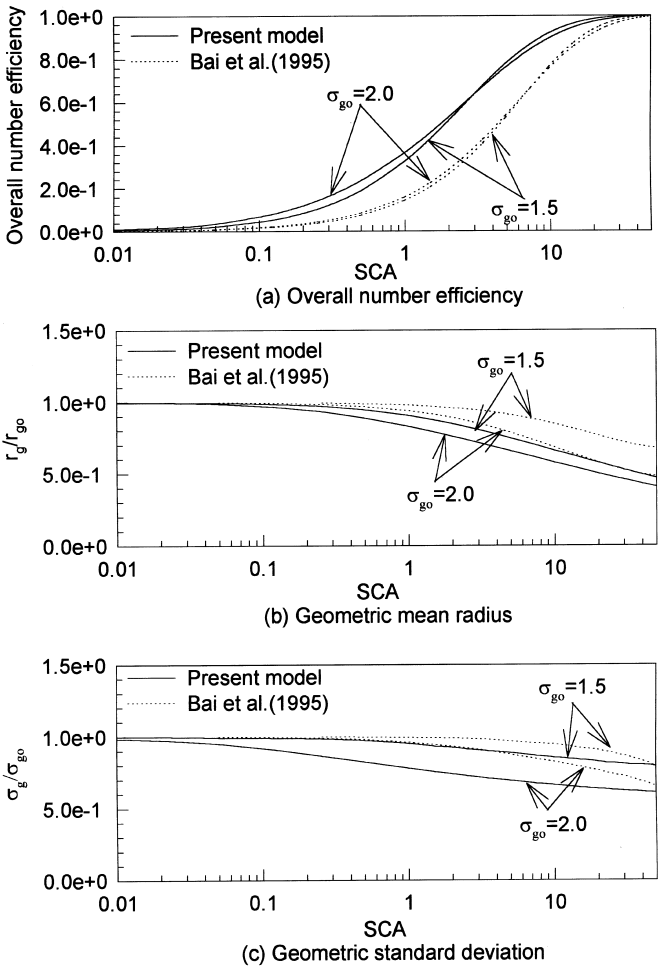


Fig. 4. Evolution of overall number efficiency, $r_g$ and $\sigma_g$ as a function of SCA for inlet particle geometric mean radius of 1 μm with different $\sigma_{g0}$ values.

coarse particles and extremely fine particles are easily precipitated, while normally fine particles are not. Eventually, the inlet particles with narrow spread have a high overall number efficiency at large SCA values, no matter whether the inlet particle geometric mean diameter ($GMD_0$) is large or small. Fig. 4(b) and (c) show the evolutions of $r_g$ and $\sigma_g$ as a function of SCA for inlet particles with different $\sigma_{g0}$ values. Both $r_g$ and $\sigma_g$ drop quickly as particles enter into an ESP, and then the rate of change of $r_g$ and $\sigma_g$ slows down. It is because both very large and very small particles are captured almost immediately after entering an ESP. The evolutions of $r_g$ and $\sigma_g$ of present model drop more quickly than those of Bai et al. model [5], because particle deposition is enhanced by particle diffusion process [7]. Fig. 5 shows the evolution of

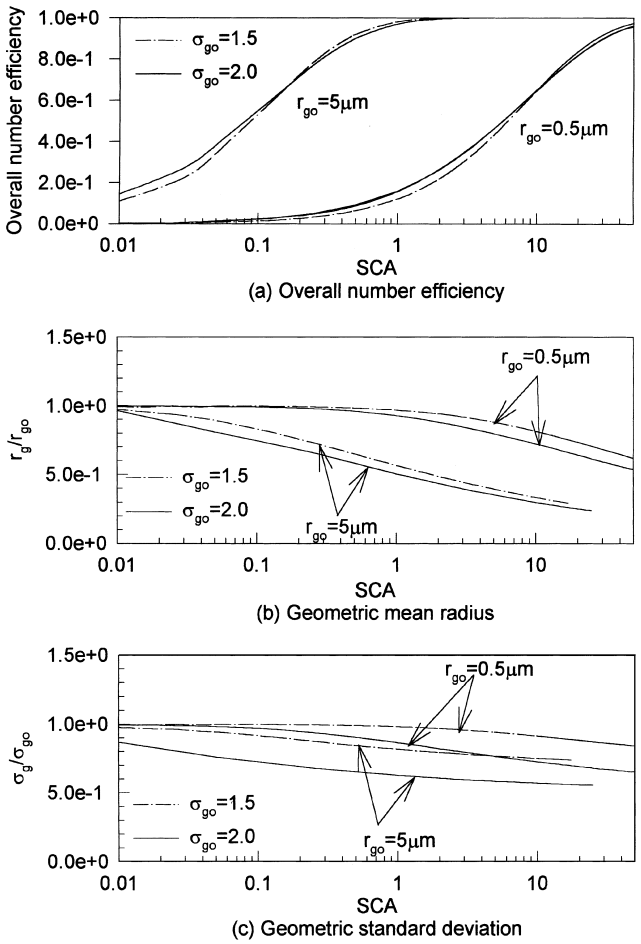


Fig. 5. Evolution of overall number efficiency, $r_g$ and $\sigma_g$ as a function of SCA predicted by present model for inlet particle geometric mean radius of 0.5 and 5 μm with different $\sigma_{g0}$ values.

overall number efficiency, $r_g$, and $\sigma_g$ as a function of SCA predicted by the present model for different particle geometric mean radius of 0.5 and 5 μm with different $\sigma_{g0}$ values. As can be seen, the overall number efficiencies are higher for inlet particles with a larger geometric mean diameter and a lower geometric standard deviation at large SCAs. Fig. 6 shows the measured and predicted results on the change of mass efficiencies at varying conditions of air velocity against incremental precipitator length. Symbols represent the measured data by Salcedo and Munz [13] while the lines represent the predicted results of the present theoretical model. The experimental conditions are summarized as follows: the electrostatic precipitator is of the wire–plate geometry with a plate-to-plate spacing of 16.2 cm, a height of 38 cm and a length of 253 cm. Discharge electrodes are placed 15.2 cm apart. Radius of the

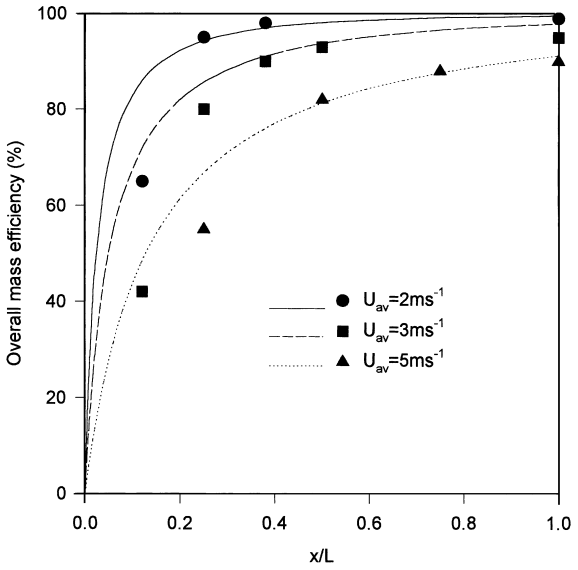


Fig. 6. Comparison of overall mass efficiency predicted by present model with published experimental data [13] (applied voltage was 38 kV).

corona wire is 0.06 cm. The applied voltages are 30 and 38 kV that provide the average values of current density at the collecting plate of $3.87 \times 10^{-4}$ and $12.8 \times 10^{-4}\,\mathrm{A\,m^{-2}}$ and the average electric field strength of 2.12 and $2.68\,\mathrm{kV\,cm^{-1}}$, respectively [11]. The experimental dust was commercial MgO particles with approximately spherical shape and the particle size distribution of MgO is well described by a lognormal function. The MgO particles have the following characteristics: the density is $3600\,\mathrm{kg\,m^{-3}}$, the electrical resistivity is $2 \times 10^{8}\,\Omega\,\mathrm{m}$, the dielectric constant is 3.4, the initial particle geometric mean diameter ($GMD_0$) is 1.5 μm and the initial geometric standard deviation ($GSD_0$) is 1.76. It is seen that experimental data are in good agreement with the predicted results at the applied voltage of 38 kV. Fig. 7 shows the comparison of experimental results with theoretical predictions at applied voltages of 30 and 38 kV. As can be seen, the present model provides a better prediction of the measured mass efficiency than that given by the other theoretical models. The measured mass efficiencies are significantly under-predicted by the Deutsch–Anderson model [1]. The Leonard et al. [3] and Zhibin and Guoquan [4] models calculated the overall mass efficiency by computing the grade efficiency over the entire particle size range and then integrating the grade efficiency to obtain the overall mass efficiency. Leonard et al. [3] and Zhibin and Guoquan [4] models over-predict the experimental data over all incremental precipitator length. The overall mass efficiencies predicted by the Bai et al. [5] and the present models remarkably improve the predicted results of Deutsch–Anderson [1] and Leonard et al. [3] models indicating that the influence of continuous change of particle size distribution may play an important role in the prediction of ESP performance. The predictions of the present

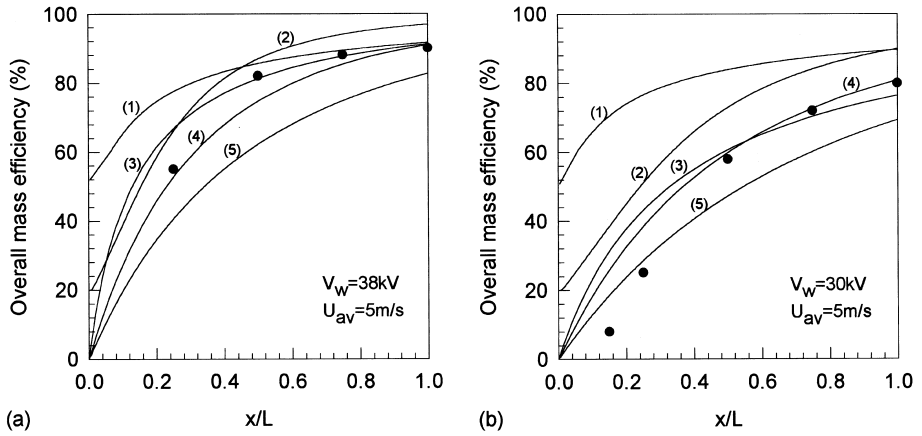


Fig. 7. Comparison between predicted mass efficiencies from other theoretical models and experimental data at different applied voltages (a) $V_w = 38\,\text{kV}$, $U_{av} = 5\,\text{m s}^{-1}$, (b) $V_w = 30\,\text{kV}$, $U_{av} = 5\,\text{ms}^{-1}$. (1) Zhibin and Guoquan [4], (2) Leonard et al. [3], (3) present model, (4) Bai et al. [5]; (5) Deutsch [1] and published experimental data [13].

model have better agreement with experimental results at a given applied voltage distribution.

## 4. Conclusions

A modified moment–lognormal model is developed to predict the continuous change of particle size distribution for considering flow convection, electrostatic force and particle diffusion process in a wire–plate ESP. The present model provides a better prediction of the experimental data of Salcedo and Munz [13] than that predicted by other theoretical prediction models including Deutsch–Anderson [1], Leonard et al. [3], Zhibin and Guoquan [4], and Bai et al. [5] models. Evolution of particle size distribution along the ESP was investigated by utilizing lognormal particle size distribution. The effects of particle size distribution of $r_g$ and $\sigma_g$ on the ESP performance were examined and quantitatively determined. The advantages of the present model lie in the fact that it considers the continuous change of the particle size distribution along an ESP and predicts both the overall mass and number efficiencies of polydisperse particles without computing the grade efficiency of each size regime. However, it must be recognized that the predictions of present model are limited to the ESPs designed and operated under the condition of low electro- and hydro-dynamic flow effects. More comprehensive data are needed for use in the validation of the present model before its practical application.

## Acknowledgements

This work was supported by the Brain Korea 21 program supported by Korean Ministry of Education.

## References

[1] W. Deutsch, Bewegung und Ladung der Elektrizitatstrager im Zylinderkondensator, Ann. Phys. 68 (1922) 335–344.
[2] G. Cooperman, A unified efficiency theory for electrostatic precipitators, J. Atmos. Environ. 18 (2) (1984) 277–285.
[3] G. Leonard, M. Mitchner, S.A. Self, Particle transport in electrostatic precipitators, J. Atmos. Environ. 14 (1980) 1289–1299.
[4] Z. Zhibin, Z. Guoquan, New model of electrostatic precipitation efficiency accounting for turbulent mixing, J. Aerosol Sci. 23 (2) (1992) 115–121.
[5] H. Bai, C. Lu, C.L. Chang, A model to predict the system performance of an electrostatic precipitator for collecting polydisperse particles, J. Air Waste Management Assoc. 45 (1995) 908–916.
[6] J.R. McDonald, W.B. Smith, H.W. Spencer III, A mathematical model for calculating electrical conditions in wire-duct electrostatic precipitation devices, J. Appl. Phys. 48 (1977) 2231–2243.
[7] K.D. Kihm, Effects of nonuniformities on particle transport in eletrostatic precipitators, Topical Report T-258, Standford University, 1987.
[8] F.M. White, Fluid Mechanics, McGraw-Hill, New York, 1986.
[9] K.H. Yoo, J.S. Lee, M.D. Oh, Charging and collection of submicron particles in two-stage parallel-plate electrostatic precipitators, Aerosol Sci. & Tech. 27 (1997) 308–323.
[10] H. Bai, P. Biswas, Deposition of lognormally distributed aerosols accounting for simultaneous diffusion, Thermophoresis and Coagulation, J. Aerosol Sci. 21 (1990) 629–640.
[11] J. Benitez, Process Engineering and Design for Air Pollution Control, Prentice-Hall, Englewood Cliffs, NJ, 1993.
[12] K.W. Lee, H. Chen, J.A. Gieseke, Log-normally preserving size distribution for Brownian coagulation in the free molecular regime, Aerosol Sci. Technol. 3 (1984) 53–62.
[13] R. Salcedo, R.J. Munz, The effect of particle shape on the collection efficiency of laboratory-scale precipitators, Proceedings of the Third International Conference on Electrostatic Precipitation, Abano-Padova, Italy, 1978, pp. 343–359.